

# An investigation of denoising parameters choice in two Perona-Malik models

Andrey Nasonov, Nikolay Mamaev, Andrey Krylov  
*Laboratory of Mathematical Methods of Image Processing*  
*Faculty of Computational Mathematics and Cybernetics*  
*Lomonosov Moscow State University*  
Moscow, Russia  
nasonov@cs.msu.ru

**Abstract**—The paper addresses the problem of no-reference parameter choice for image denoising by Perona-Malik image diffusion algorithm using two models. The idea of the approach is to analyze the difference image between noisy input image and the outcome of the denoising algorithm for the presence of structured data from the input image. The analysis consists of the calculation of the mutual information — a value that shows the ratio between the structured data and the noise. We apply the proposed method to photographic images, vector graphics images and to retinal images with modeled Gaussian noise with different parameters.

**Index Terms**—Image denoising, mutual information, Perona-Malik diffusion, automatic parameter choice.

## I. INTRODUCTION

Image denoising is one of the most important problems in image processing. Noisy images appears everywhere. Images are often corrupted by noise during acquisition, transmission or storage. The goal of image denoising is to restore the original image by removing the noise while preserving the original data. Image denoising is often applied as a preparation step before using other image processing methods. A great research effort has been done for image denoising, but the problem still remains unsolved.

Most image denoising algorithms depend on noise level and thus must be controlled by parameters entered by a user or estimated automatically. A common approach for automatic choice of the parameters is to estimate the noise level and then choose the parameters according to this noise level [1].

A less common approach is to analyze the preservation of image contents after image denoising with different parameters and to pose the stopping criterion. For example, the work [2] analyzes the edge characteristics, the work [3] calculates image statistics for speckle noise reduction. The method [4] analyzes the difference between the original noisy image and the processed image. Its idea comes from an assumption that the noise is unstructured, so in the ideal case the difference image must contain just random values without any structures from the original image. The presence of structures in the difference images indicates that we have wiped out some important information as well as the noise.

In this paper, we investigate the automatic choice of the parameters for non-linear diffusion method proposed in [5] by Perona and Malik. The diffusion method represents a denoised image as a solution of nonlinear diffusion equation with the original image as initial state and homogeneous Neumann boundary conditions. By choosing the diffusion parameter, one can manage to clean flat areas and preserve edges. Non-linear diffusion is an iterative process so there is a stop criterion problem.

## II. PERONA-MALIK IMAGE DIFFUSION

One of the methods for image denoising is based on non-linear diffusion. The clean image is considered as the solution of the heat conduction. The diffusion coefficient map is chosen in order to reduce the diffusivity in edges areas. Such methods allow to preserve edges during denoising due to the proper choice of coefficient. Koenderink [6] and Hummel [7] pointed out that an imaged convolved with the Gaussian kernel can be viewed as the solution of the heat conduction equation with original image as initial condition.

$$\begin{aligned}\frac{\partial u}{\partial t} &= \operatorname{div}(c\nabla u), \quad (x, t) \in \Omega \times [0, T], \\ u(x, 0) &= l_0, \quad x \in \Omega, \\ \frac{\partial u}{\partial \vec{n}} &= 0, \quad (x, t) \in \partial\Omega \times [0, T],\end{aligned}$$

where  $l_0$  is the input image defined in spatial domain  $\Omega$ ,  $c$  is the diffusion coefficient,  $u(x, T)$  is the result of heat distribution at moment  $T$ .

In linear diffusion the coefficient  $c$  is considered to be constant and independent of the image. In non-linear diffusion, the coefficient  $c$  is a function of image gradient magnitude  $c = c(|\nabla u|)$ , which controls the blurring effect. Setting  $c$  to 1 in interior of each region and 0 at the boundaries will encourage smoothing within a region and stop it on the edge, so that the boundaries remain sharp. In [5] Perona and Malik proposed the following two functions as edge estimator:

$$c_1(s) = \exp\left(-\left(\frac{s}{K}\right)^2\right) \quad (1)$$

and

$$c_2(s) = \frac{1}{1 + \left(\frac{s}{K}\right)^2}, \quad (2)$$

where  $K$  is the parameter of the method.

The diffusion equation can be solved iteratively by simple step algorithm:

$$\begin{aligned} u_{n+1} &= u_n + t_n \cdot c(|\nabla u|) \Delta u, \\ u_0 &= u(x, 0) = I_0, \\ \sum_n t_n &= T. \end{aligned}$$

### III. TARGET IMAGES

We have analyzed the automatic choice of the parameters for the Perona-Malik image diffusion algorithm for both models (1) and (2) for images of the following three classes:

- Photographic images from TID database [8];
- Retinal images from DRIVE database [9];
- Synthetic bubbles image with Gaussian blur with various blur level within  $[0, 5]$  range.

An example of those images is shown in Fig. 1.

In order to model noisy images, we have added white Gaussian noise to the reference images. For each reference image, we have generated 20 noisy images with random standard deviation of Gaussian noise  $\sigma$  within  $[1, 32]$  range.

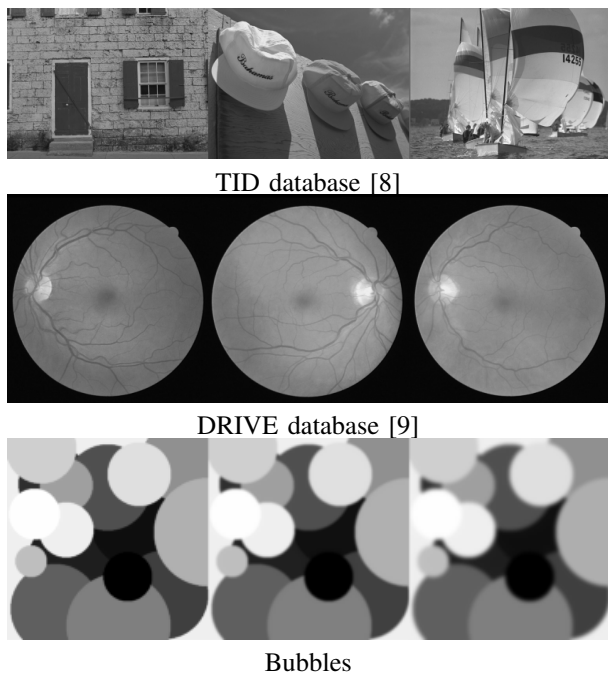


Fig. 1. An example of reference images used for the analysis in the paper.

### IV. FULL-REFERENCE PARAMETER ANALYSIS

For each noisy image, we have obtained a pair of  $(K, T)$  parameters that maximizes PSNR and SSIM [10] metric values. We have found that for each image there is a set of  $(K, T)$  values producing the results that are almost indistinguishable

from the optimal result. The set is banana-shaped and lies perpendicular to the line passing through the zero point. Fig. 2 shows an example of optimal  $(K, T)$  values for one of the images for different noise levels.

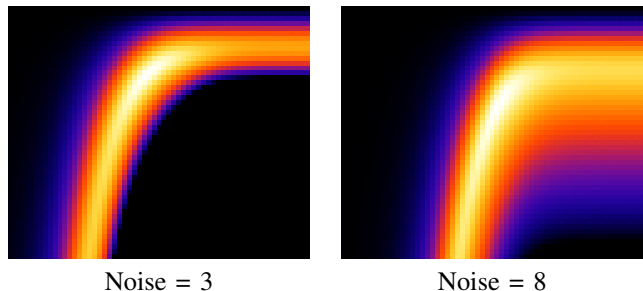


Fig. 2. A visualization of optimal  $(K, T)$  parameters maximizing PSNR for an image with different noise levels (Gaussian noise,  $\sigma = 3$  and  $\sigma = 8$ ). The horizontal axis represents  $K + 1$  value in logarithmic scale. The vertical axis represents  $T$  value. Top-left corner is  $(0, 0)$  point. White regions corresponds to  $(K, T)$  values that produce images with PSNR values close to the optimal value. Black regions correspond to PSNR values equal or less than PSNR for the unprocessed image.

We have also noticed that for each noise level the ratio  $K/T$  can be fixed yielding one-dimensional parameter optimization, but for different noise level the optimal ratio  $K/T$  set is different.

In order to go from two-dimensional to one-dimensional parameter optimization for any noise level, we have analyzed the behavior of optimal  $(K, T)$  values and have found out that a set of optimal points  $(\log K, \sqrt{T})$  lies along a line. Therefore, we introduce single-argument parameterization for  $(K, T)$  values:

$$\begin{aligned} K &= q_1 q_2^p, \\ T &= p^2, \end{aligned} \quad (3)$$

where the coefficients  $q_1$  and  $q_2$  are chosen experimentally by optimizing the full-reference metrics values.

For both TID, DRIVE and bubbles images, we have fixed  $q_1 = 0.1$  and optimized  $q_2$  value. The ranges of optimal values for different image classes are different, but they intersects. We have chosen  $q_2 = 4600$  from the intersection.

### V. NO-REFERENCE PARAMETER CHOICE

We use the algorithm [4] for no-reference parameter choice. The algorithm is based on the assumption that the difference between input noisy and denoised images should not have features belonging to original image. In order to detect the presence of these features, the algorithm analyses the eigenvalues of Hessian matrix for scale and direction evaluation of ridges and edges. The outcome of the algorithm is value  $\mu$  — the mutual information that can be expressed as the structure-to-noise ratio for the difference image. The lower the value  $\mu$  is, the less details are corrupted compared to noise removal.

We use the following scenario: an image denoising algorithm is executed with different parameters, then the mutual information  $\mu$  value is calculated between the input image and each denoising result, and the image that minimizes the mutual

information is chosen as the optimal result. In practice, there can be several local minima, and a special analysis should be performed in order to choose the optimal result.

After replacing the two-parameter model with the single-parameter model (3), we find the optimal  $p$  value using both full-reference and no-reference approach based on calculating the mutual information coefficient.

It has been found that mutual information correlates well with PSNR and SSIM values for noise level  $\sigma > 2$ . An example is shown in Fig. 3. A argument where PSNR and/or SSIM reaches its maximum is close to a local minimum of  $\mu(p)$  function. In the case of several local minima points, we find the one that maximizes the drop:

$$p_{opt} = \arg_p \max_{p' < p} \mu(p') - \mu(p). \quad (4)$$

In the case of very low noise level ( $\sigma \leq 2$ ), the method has limited application. Non-linear diffusion improves the image very little in the case of low noise. The difference image has low magnitude, so the mutual information coefficient is low, and local minimum point becomes unstable or even disappears.

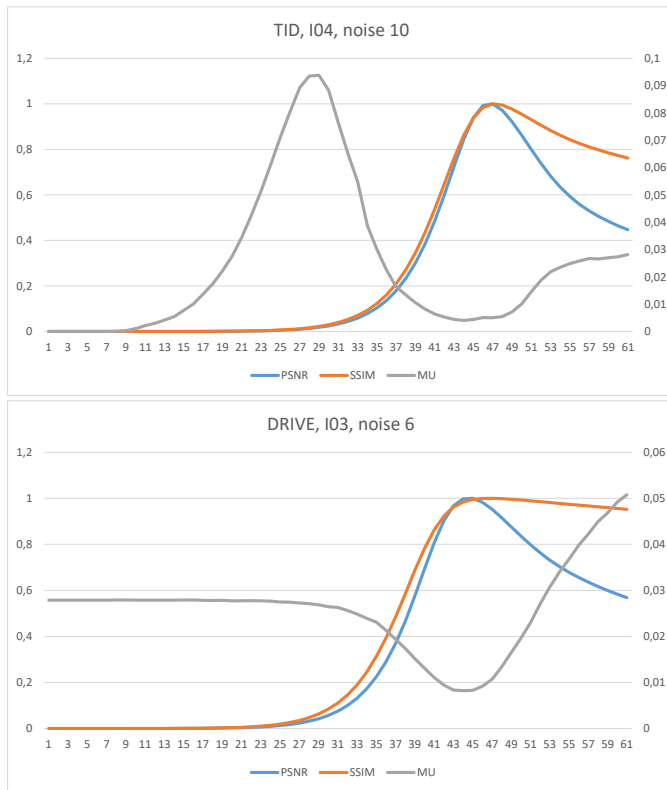


Fig. 3. Examples of the dependence of PSNR, SSIM and mutual information on the parameter  $p$  corresponding to denoising strength. The PSNR and SSIM values are normalized into  $[0, 1]$  range by a linear transform.

## VI. RESULTS

The numerical results for different scenarios of denoising parameter choice for the models EXP (1) and DIV (2) are presented in Fig. 4 and Fig. 5. The results are averaged for all the images with noise level  $\sigma > 2$ .

Despite the fact that the proposed no-reference algorithm has worse PSNR and SSIM values than the optimal ones, the difference between the results of the proposed algorithm and the optimal results is practically indistinguishable, and the effectiveness of image denoising is clearly visible. Also, for most of the images there is no difference between models (1) and (2). For some images with sharp edges and strong noise, the model (1) produces salt-and-pepper noise artifacts (see Fig. 6). This results in better average PSNR and SSIM values for the model (2).

The individual results are shown in Fig. 7, Fig. 8 and Fig. 9.

## VII. CONCLUSION

The paper has shown that the parameters of the Perona-Malik image denoising algorithm can be automatically and effectively chosen by the algorithm that analyzes the presence of structures from the input image in the difference image.

## REFERENCES

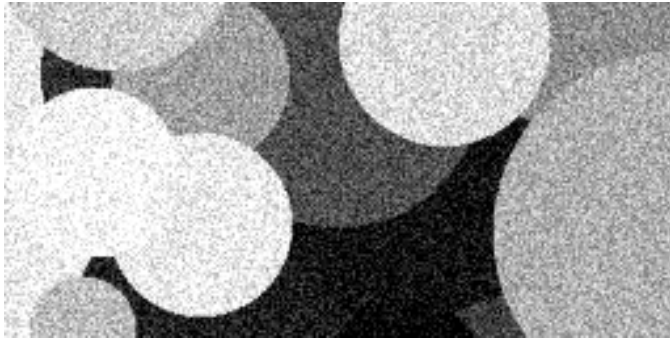
- [1] Karl Krissian and Santiago Aja-Fernández. Noise-driven anisotropic diffusion filtering of mri. *IEEE transactions on image processing*, 18(10):2265–2274, 2009.
- [2] Chourmouzios Tsiotsios and Maria Petrou. On the choice of the parameters for anisotropic diffusion in image processing. *Pattern recognition*, 46(5):1369–1381, 2013.
- [3] Santiago Aja-Fernández and Carlos Alberola-López. On the estimation of the coefficient of variation for anisotropic diffusion speckle filtering. *IEEE Transactions on Image Processing*, 15(9):2694–2701, 2006.
- [4] Nikolay Mamaev, Dmitry Yurin, and Andrey Krylov. Choice of the parameter for bm3d denoising algorithm using no-reference metric. In *2018 7th European Workshop on Visual Information Processing (EUVIP)*, pages 1–6. IEEE, 2018.
- [5] Pietro Perona and Jitendra Malik. Scale-space and edge detection using anisotropic diffusion. *IEEE Transactions on pattern analysis and machine intelligence*, 12(7):629–639, 1990.
- [6] Jan J Koenderink. The structure of images. *Biological cybernetics*, 50(5):363–370, 1984.
- [7] Robert A Hummel. Representations based on zero-crossings in scale-space. In *Readings in Computer Vision*, pages 753–758. Elsevier, 1987.
- [8] N. Ponomarenko, L. Jin, O. Ieremeiev, V. Lukin, K. Egiazarian, J. Astola, B. Vozel, K. Chehdi, M. Carli, F. Battisti, and C.-C. Jay Kuo. Image database tid2013: Peculiarities, results and perspectives. *Signal Processing: Image Communication*, 30:57–77, 2015.
- [9] M.D. Abramoff J.J. Staa and, M. Niemeijer, M.A. Viergever, and B. van Ginneken. Ridge based vessel segmentation in color images of the retina. *IEEE Transactions on Medical Imaging*, 23:501–509, 2004.
- [10] Z. Wang, A. Bovik, H. Sheikh, and E. Simoncelli. Image quality assessment: from error visibility to structural similarity. *IEEE Transactions on Image Processing*, 13(4):600–612, 2004.

Optimization method	TID		DRIVE		Bubbles	
	EXP	DIV	EXP	DIV	EXP	DIV
Input noisy images	29.95	29.95	29.86	29.86	31.09	31.09
Full-reference, double-parameter, by PSNR	33.73	33.85	38.55	38.65	40.10	40.39
Full-reference, double-parameter, by SSIM	33.51	33.66	38.08	38.16	38.59	39.12
Full-reference, single-parameter, by PSNR	33.70	33.62	38.33	38.26	39.51	39.65
Full-reference, single-parameter, by SSIM	33.44	33.58	37.61	37.66	37.87	38.46
No-reference, single-parameter, by MU (proposed)	33.35	33.41	38.31	38.39	39.94	40.20

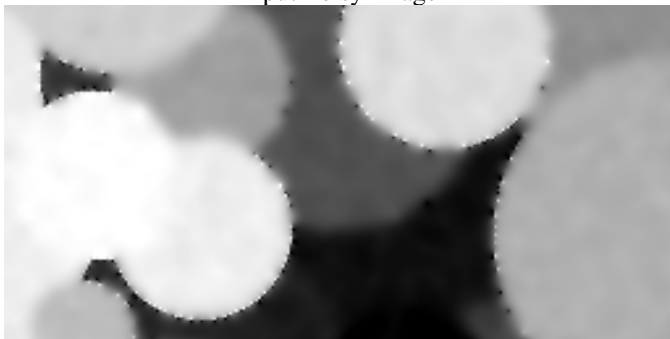
Fig. 4. PSNR results for anisotropic diffusion model for images of different classes.

Optimization method	TID		DRIVE		Bubbles	
	EXP	DIV	EXP	DIV	EXP	DIV
Input noisy images	0.7626	0.7626	0.5758	0.5758	0.6969	0.6969
Full-reference, double-parameter, by PSNR	0.9018	0.9043	0.9121	0.9138	0.9532	0.9576
Full-reference, double-parameter, by SSIM	0.9090	0.9102	0.9225	0.9229	0.9712	0.9730
Full-reference, single-parameter, by PSNR	0.8997	0.9023	0.9052	0.9065	0.9487	0.9521
Full-reference, single-parameter, by SSIM	0.9074	0.9085	0.9180	0.9183	0.9660	0.9684
No-reference, single-parameter, by MU (proposed)	0.8972	0.9001	0.9105	0.9110	0.9519	0.9533

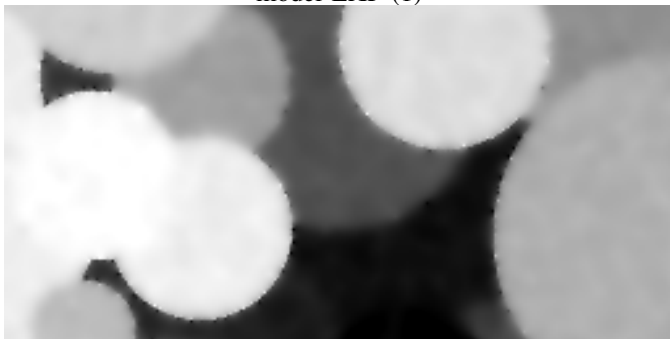
Fig. 5. SSIM results for anisotropic diffusion model for images of different classes.



Input noisy image



The result of denoising using non-linear diffusion with model EXP (1)



The result of denoising using non-linear diffusion with model DIV (2)

Fig. 6. Denoising by the proposed method. Bubbles image I00, noise  $\sigma = 25$ .

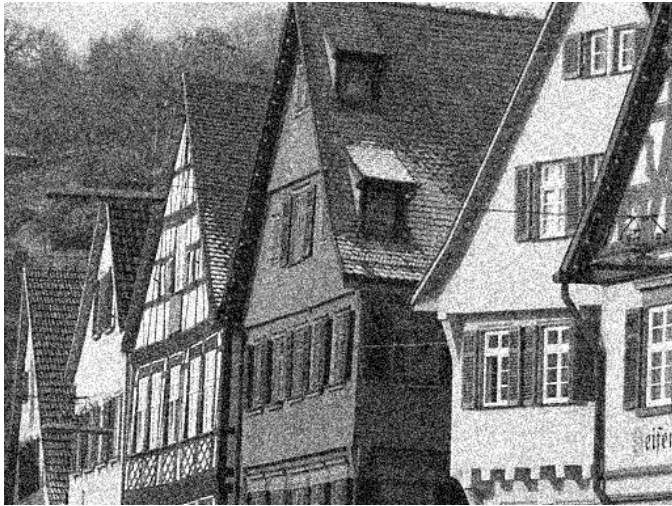


Input noisy image

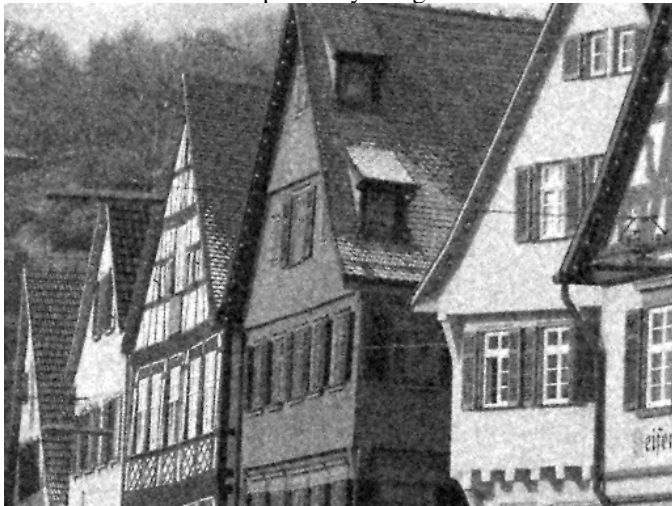


The result of denoising using non-linear diffusion

Fig. 7. Denoising by the proposed method. TID image I07, noise  $\sigma = 4$ .

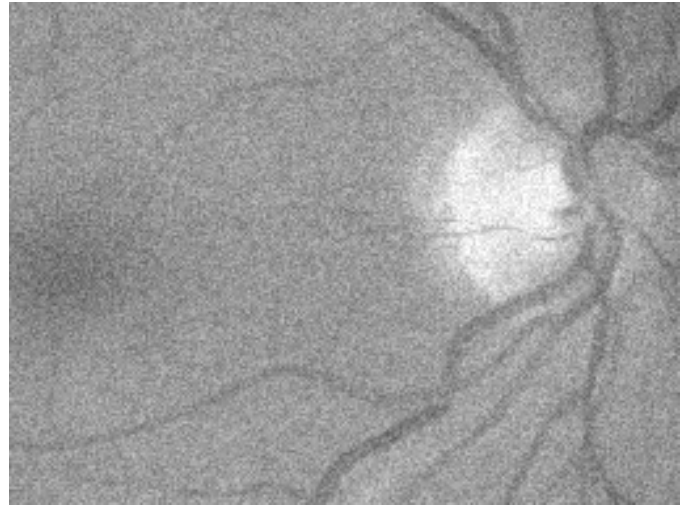


Input noisy image

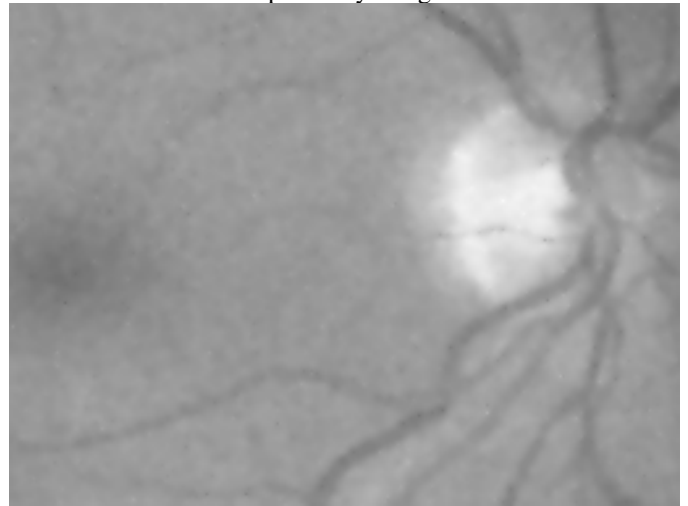


The result of denoising using non-linear diffusion

Fig. 8. Denoising by the proposed method. TID image I08, noise  $\sigma = 32$ .



Input noisy image



The result of denoising using non-linear diffusion

Fig. 9. Denoising by the proposed method. DRIVE image I02, noise  $\sigma = 13$ .